

CHARACTERIZATION OF GRAPHENE OXIDE
PICKERING EMULSION AND SILICA
NANOPARTICLES FOR
WATERBORNE EPOXY
COATING

BY

NURUL NADIAH BINTI SAHIR

A thesis submitted in fulfilment of the requirement for the
degree of Master of Science (Materials Engineering)

Kulliyyah of Engineering
International Islamic University Malaysia

OCTOBER 2020

ABSTRACT

The application of epoxy resins as the anticorrosion coating has obtained widespread application because of their superior adhesion to various substrate and excellent chemical inertness. However, epoxy resin tends to form microcracks and the VOCs released during the drying process is harmful. Although the waterborne epoxy coatings are a much safer alternative, they are prone to swell caused by water absorption. With the consideration for the environment and human health in mind, this research aimed at developing a new and improved waterborne coating that employed graphene oxide (GO) encapsulated linseed oil and silica nanoparticles (SiO_2) as healing microcapsules and anticorrosion agent respectively. This research was divided into three main phases; phase (A), synthesis of graphene oxide microcapsules (GOMs) via Pickering emulsion method, phase (B), synthesis of amine-stitched graphene oxide microcapsules (Amine-stitched GOMs), and phase (C), preparation of coating sample. GO was selected as the microcapsule's shell due to its flexibility and excellent barrier properties, while the linseed oil core is able to polymerize when in contact with the atmosphere to form a hydrophobic film. SiO_2 was used to increase the density and adhesion between the coating and the substrate. This coating was formulated through the copolymerization of waterborne epoxy resin with the incorporation of GOMs and SiO_2 nanoparticles. Waterborne epoxy acted as a matrix while GOMs and SiO_2 nanoparticles act as a guest component. The coating was directly applied on carbon steel type S50C as the substrate. The test of adhesion, immersion, and salt spray was conducted in accordance with ASTM D3359, B895, and B117-94 respectively. The POM, TGA, and TEM showed that the GOMs were successfully synthesized, having a size ranging from 5.39 μm to 20.45 μm , coefficient of variation (Cv) of 0.34, shell thickness around 140 to 160 nm, and 94% loading capacity. Based on the physical analysis and corrosion test, the addition of GOMs and SiO_2 nanoparticles reduced the swelling degree and corrosion rate of a waterborne epoxy coating by 54.1% and 62.7% respectively. The novel formulated coating also demonstrated good adhesion to the metal substrate and possess the ability to perform as a self-healing coating. Incorporation of 10 wt% GOMs and 1 wt% of SiO_2 nanoparticles were identified as the best composition for waterborne epoxy coating in improving waterborne coating properties.

خلاصة البحث

قد حصلت مادة الإيبوكسي التي تستخدم كطلاء لمنع التآكل على إستعمال واسع بسبب قوة التصاقها المتفوق لمختلف المواد المتفاعلة والمواد الخاملة كيميائياً. ومع ذلك، مادة الإيبوكسي تميل إلى تشكيل شقوق صغيرة والمركبات العضوية المتطايرة المنبعثة أثناء عملية التجفيف تكون مضرّة. ورغم أن طلاءات الإيبوكسي المائية تعتبر بديلاً أكثر أماناً، ولكنها أكثر عرضة للتضخم بسبب إمتصاص الماء. يهدف هذا البحث في تطوير الطلاء المائي بشكل جديد ومحسن مع الأخذ بعين الإعتبار البيئة المحيطة وصحة الإنسان، والذي يستخدم أكسيد الجرافين (GO) المغلف بزيت بذر الكتان وجزئيات السيليكون (SiO_2) ككبسولات شفاء وعامل مضاد للتآكل. وينقسم هذا البحث إلى ثلاثة مراحل: المرحلة الأولى (A)، توليف كبسولات أكسيد الجرافين (GOMs) على طريقة مستحلب بيكرينغ. المرحلة الثانية (B)، توليف كبسولات أكسيد الجرافين المخيطة بالأمين (Amine-stitched GOMs). وأما المرحلة الثالثة (C)، هي تجهيز عينات الطلاء. وتم اختيار أكسيد الجرافين كغلاف للكبسولات بسبب مرونتها ومناعتها الممتازة، بينما نواة بذرة الكتان قادرة على التبلمر عندما تتصل بالغللاف الجوي لتشكل غشاء الهيدروفوبيك. كان يستخدم ثاني أكسيد السيليكون لزيادة شدة وقوة التصاق بين الطلاء والمادة المتفاعلة. هذا الطلاء قد صيغ عن طريق البلمرة من مادة الإيبوكسي المائي ودمجه مع كبسولات أكسيد الجرافين ونانويات ثاني أكسيد السيليكون. ويعمل الإيبوكسي المائي كنسيج غشائي، بينما كبسولات أكسيد الجرافين ونانويات ثاني أكسيد السيليكون يعملون كعنصر مضيف. ويستعمل الطلاء مباشرة على الكربون الصلب من نوع S50C كمادة متفاعلة. تم إختبار سلوك كل من الإلتصاق، الإنغمار ورذاذ الملح وفقاً لـ ASTM D3359, B895, و B11794 بالتوالي. أظهرت الـ POM, TGA, و TEM أن كبسولات أكسيد الجرافين قد تم توليفها بنجاح، مع وجود أحجام تتراوح ما بين 5.39 ميكرومتر. و 0.34 من معامل الإختلاف. وسماكة القشرة تتراوح ما بين 140 إلى 160 نانومتر، و 94 بالمئة من قدرة التحميل. وبناء على التحليل الفيزيائي وإختبار التآكل، الزيادة في كبسولات أكسيد الجرافين وثاني أكسيد السيليكون قلصت درجة الإنتفاخ ونسبة تآكل طلاء الإيبوكسي المائي، بنسبة 54.1 بالمئة و 62.7 بالمئة على التوالي. الطلاء المطور حديثاً قد برهن خصائص إلتصاق جيد على الركيزة المعدنية وامتلاكه القدرة على الإستشفاء الذاتي. طلاء الإيبوكسي المائي المكون من 10 بالمئة من سمك حائط كبسولات أكسيد الجرافين و 1 بالمئة من سمك حائط نانويات ثاني أكسيد السيليكون يعتبر أفضل تركيب لطلاء الإيبوكسي المائي في مجال تطوير الطلاءات المائية.

APPROVAL PAGE

I certify that I have supervised and read this study and that in my opinion, it conforms to acceptable standards of scholarly presentation and is fully adequate, in scope and quality, as a thesis for the degree of Master of Science (Materials Engineering).

.....
Noor Azlina Binti Hassan
Supervisor

.....
Norita Binti Hassan
Co-Supervisor

.....
Noorasikin Binti Samat
Co-Supervisor

I certify that I have read this study and that in my opinion it conforms to acceptable standards of scholarly presentation and is fully adequate, in scope and quality, as a thesis for the degree of Master of Science (Materials Engineering).

.....
Norshahida Binti Sarifuddin
Internal Examiner

.....
Sahrim Bin Hj. Ahmad
External Examiner

This thesis was submitted to the Department of Manufacturing and Materials Engineering and is accepted as a fulfilment of the requirement for the degree of Master of Science (Materials Engineering).

.....
Mohamed bin Abdul Rahman
Head, Department of
Manufacturing and Materials
Engineering

This thesis was submitted to the Kulliyah of Engineering and is accepted as a fulfilment of the requirement for the degree of Master of Science (Materials Engineering)

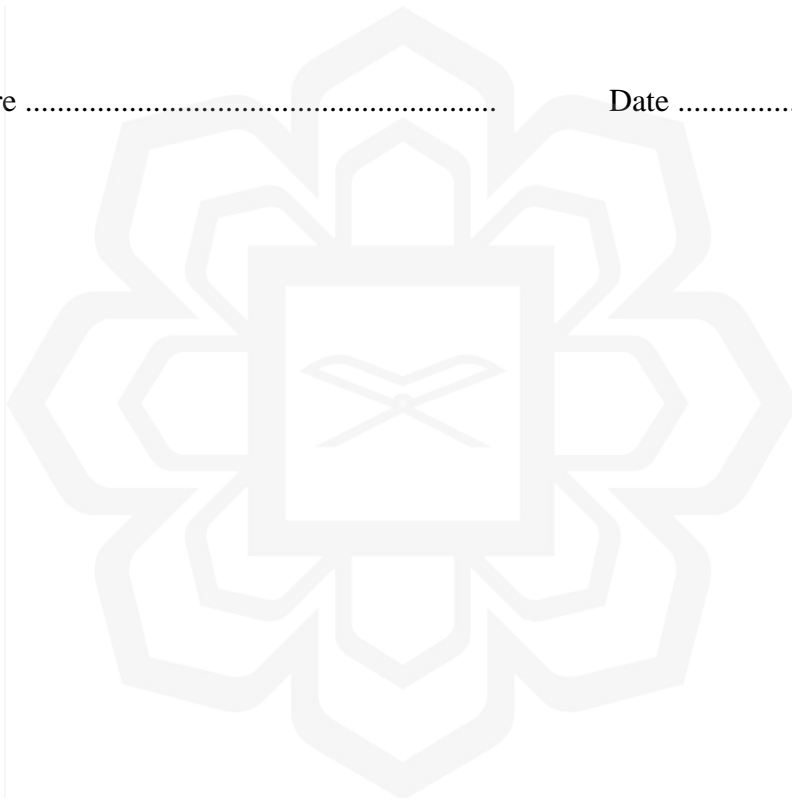
.....
Sany Izan Ihsan
Dean, Kulliyah of Engineering

DECLARATION

I hereby declare that this thesis is the result of my own investigations, except where otherwise stated. I also declare that it has not been previously or concurrently submitted as a whole for any other degrees at IIUM or other institutions.

Nurul Nadiah Binti Sahir

Signature Date



INTERNATIONAL ISLAMIC UNIVERSITY MALAYSIA

**DECLARATION OF COPYRIGHT AND AFFIRMATION OF
FAIR USE OF UNPUBLISHED RESEARCH**

**CHARACTERIZATION OF GRAPHENE OXIDE PICKERING
EMULSION AND SILICA NANOPARTICLES FOR
WATERBORNE EPOXY COATING**

I declare that the copyright holder of this thesis are jointly owned by the student and IIUM.

Copyright © 2020 Nurul Nadiah Binti Sahir and International Islamic University Malaysia. All rights reserved.

No part of this unpublished research may be reproduced, stored in a retrieval system, or transmitted, in any form or by any means, electronic, mechanical, photocopying, recording or otherwise without prior written permission of the copyright holder except as provided below

1. Any material contained in or derived from this unpublished research may be used by others in their writing with due acknowledgement.
2. IIUM or its library will have the right to make and transmit copies (print or electronic) for institutional and academic purposes.
3. The IIUM library will have the right to make, store in a retrieved system and supply copies of this unpublished research if requested by other universities and research libraries.

By signing this form, I acknowledged that I have read and understand the IIUM Intellectual Property Right and Commercialization policy.

Affirmed by Nurul Nadiah Binti Sahir

.....
Signature

.....
Date

ACKNOWLEDGEMENTS

In the Name of Allah, the Most Gracious, the Beneficent, and the Most Merciful. First praise is to Allah, the Almighty, on whom ultimately we depend for sustenance and guidance.

I would like to thank my supervisor, Assoc. Prof. Dr. Noor Azlina Hassan. The door to her office was always open whenever I ran into a trouble spot or had a question about my research or writing. She consistently allowed this paper to be my own work but steered me in the right direction whenever she thought I needed it. I could not have imagined having a better advisor for my Masters's study. Not forgotten, Dr. Norita Hassan, Dr. Norhasnidawani Johari, and Assoc. Prof. Dr. Noorasikin Samat for their support and knowledge regarding this topic.

My sincere thanks also go to IIUM Materials Laboratory's staffs; who gives the permission to use all the required machinery and the necessary materials, Amir Hakimi and Atiqah Akhir; for their humor, kindness and moral support during my study, Suffian Rosli; for providing me with unfailing support and continuous encouragement throughout my years of study and through the process of researching and writing this thesis. This accomplishment would not have been possible without them. Thank you.

It is my utmost pleasure to dedicate this work to my dear parents and my family, who granted me the gift of their unwavering belief in my ability to accomplish this goal: thank you for your support and patience.

Finally, I would like to like to congratulate myself, and thank myself, and give myself a big pat on the back. Thank you Nadiah for not giving up although this journey has been rough, for able to pick up yourself when the world is against you, for being able to stand your ground when everything seems so wrong. You are the best, and I am proud of you.

TABLE OF CONTENTS

Abstract	ii
Abstract in Arabic	iii
Approval page	iv
Declaration	v
Copyright Page.....	vi
Acknowledgements	vii
Table of contents	viii
List of Tables	xi
List of Figures	xii
List of symbols.....	xvii
List of equations.....	xix
List of abbreviations	xx
CHAPTER ONE: INTRODUCTION	1
1.1 Background of The Study	1
1.2 Corrosion	2
1.2.1 Corrosion of Carbon Steel.....	3
1.2.2 Corrosion Protection	5
1.3 Problem Statement.....	6
1.4 Research Objectives.....	8
1.5 Significance of The Study	8
1.6 Scope And Limitations	9
1.7 Thesis Outline.....	9
CHAPTER TWO: LITERATURE REVIEW	11
2.1 Introduction.....	11
2.2 Smart Coating	11
2.2.1 Core.....	13
2.2.2 Shell	15
2.3 Graphene Oxide (GO).....	19
2.3.1 Structure and Morphology	21
2.3.2 Chemistry of GO	25
2.3.3 Barrier Properties of GO	28
2.3.4 Anticorrosion Properties of GO	29
2.3.5 Application: Self-Healing	31
2.4 Linseed Oil.....	32
2.4.1 Physical and Chemical Properties.....	33
2.4.2 Linseed Oil as ‘Green’ Self-healing Agent.....	34
2.5 Pickering Emulsion.....	35
2.5.1 Concentration of Solid Particles	37
2.5.2 Emulsification Energy.....	38
2.6 Filler.....	39
2.6.1 Silica Nanoparticles	40
2.7 Chapter Summary	41

CHAPTER THREE: METHODOLOGY	47
3.1 Introduction.....	47
3.2 Materials	47
3.2.1 Graphene Oxide (GO) Solution	47
3.2.2 Linseed Oil	48
3.2.3 Poly(propylene glycol) bis(2-aminopropyl ether), D2000.....	48
3.2.4 Silica Nanoparticles (SNPs).....	48
3.2.5 Waterborne Epoxy Resin and Curing Agent.....	48
3.2.6 Carbon Steel.....	49
3.3 Method.....	49
3.3.1 Raw Materials Characterization.....	49
3.3.2 Phase (A) Synthesis of Graphene Oxide Microcapsules (GOMs).....	51
3.3.3 Phase (B) Synthesis of Amine-Stitched Graphene Oxide Microcapsules (Amine-stitched GOMs).....	52
3.3.4 GOMs Characterization and Testing.....	52
3.4 Phase (C) Preparation of Coating Sample	54
3.4.1 GOMs Single Coating System	55
3.4.2 GOMs-Silica Coating System.....	56
3.5 Coating's Characterization Technique	57
3.5.1 Polarized Optical Microscope (POM).....	57
3.5.2 Fourier Transform Infrared Spectroscopy (FTIR)	57
3.5.3 X-Ray Diffractometer (XRD)	57
3.5.4 3-D Laser Scanning Microscope (3D-OM)	58
3.6 Self-Healing Testing.....	58
3.6.1 Scratch Test.....	58
3.7 Adhesion Testing	58
3.8 Corrosion Testing	59
3.8.1 Immersion Testing	59
3.8.2 Salt Spray Testing	60
3.9 Summary Of The Chapter.....	60
CHAPTER FOUR: RESULTS AND DISCUSSIONS	63
4.1 Introduction.....	63
4.2 Raw Materials Characterization	63
4.2.1 RAMAN Spectroscopy	63
4.2.2 Particle Size Analyser (PSA) Analysis	65
4.2.3 Scanning Electron Microscope (SEM) and Transmission Electron Microscope (TEM) Analysis.....	65
4.3 Phase (A) Synthesis Of Graphene Oxide Microcapsules (GOMS)	66
4.3.1 Effect of Disperse Speed.....	66
4.3.2 Effect of Concentration of Solid Particles (GO).....	75
4.3.3 Preparation of GOMs Using Optimum Parameter.....	82
4.4 Phase (B) Synthesis of Amine-Stitched Graphene Oxide Microcapsules (GOMS).....	94
4.4.1 Structural Analysis of Amine-stitched GOMs Shell.....	95
4.4.2 Stability Test	97
4.4.3 Dispersibility of Amine-stitched GOMs in Coating Matrix	98
4.5 Phase (C) Preparation Of Goms Waterborne Epoxy Coating Sample ...	101

4.5.1 Polarized Optical Microscope (POM) Analysis.....	101
4.5.2 X-Ray Diffractometer (XRD) Analysis	103
4.6 Characterization Of The GOMs Coating System	104
4.6.1 Adhesion Test	104
4.6.2 Immersion Test	105
4.6.3 Salt Spray Test (SST).....	112
4.6.4 Scratch Test.....	115
4.7 Preparation of GOMs-Silica Waterborne Epoxy Coating Sample	117
4.7.1 Polarized Optical Microscope (POM) Analysis.....	117
4.7.2 X-Ray Diffractometer (XRD) Analysis	119
4.8 Characterization Of The GOMs-Silica Coating System.....	120
4.8.1 Adhesion Test	120
4.8.2 Immersion Test	121
4.8.3 Scratch Test.....	126
CHAPTER FIVE: CONCLUSION	129
5.1 Conclusion	129
5.2 Recommendation For Future Works	130
REFERENCES.....	132
APPENDIX 1: LIST OF CONFERENCE PROCEEDING, PUBLICATION AND EXHIBITION	146
APPENDIX 2: CARBON STEEL DATASHEET.....	147

LIST OF TABLES

Table 1.1	Types of carbon steel	3
Table 2.1	Basic properties of Graphene	20
Table 2.2	Physical properties of linseed oil	33
Table 2.3	Previous researches related on GO/GOMs/Silica coating system.	42
Table 3.1	Composition of S50C carbon steel	49
Table 3.2	Emulsion prepared with varied disperse speed	51
Table 3.3	Emulsion prepared with varied GO concentration	51
Table 3.4	Coating samples prepared with varied GOMs loading	56
Table 3.5	GOMs-Silica coating samples	56
Table 4.1	ID/IG and I2D/IG ratio of GO	64
Table 4.2	Average size and Cv value for each emulsion	72
Table 4.3	Average size and Cv value for each emulsion	79
Table 4.4	Theoretical number of microcapsules, total surface area and thickness of GOMs to its respected diameter	87
Table 4.5	Adhesion percentage for WB epoxy coating with different wt% GOMs loading	105
Table 4.6	Weight difference of carbon steel samples after 720 hours immersion	108
Table 4.7	Weight loss and corrosion rate of carbon steel with different wt% GOMs loading	111
Table 4.8	Adhesion percentage for GOMs epoxy coating with different wt% silica nanoparticles	121
Table 4.9	Weight difference of coating samples after 720 hours immersion	122
Table 4.10	Weight loss and corrosion rate of carbon steel with different wt% silica loading	126

LIST OF FIGURES

Figure 1.1	Corrosion costs breakdown across industrial sectors (Kruger & Begum, 2016)	3
Figure 1.2	General scheme for various forms of corrosion in metals or alloys (Zarras & Stenger-Smith, 2014)	5
Figure 2.1	Smart materials market (Source: Zion Market Research 2017, Taken from https://www.zionmarketresearch.com/news/smart-materials-market , 29 January 2019)	12
Figure 2.2	Factor contributing to smart materials market (Source: Primary & secondary research and AMR analysis, Taken from https://www.alliedmarketresearch.com/smart-material-market , 29 January 2019)	12
Figure 2.3	The propagation of crack breaks the capsule shell, releasing the healing agent to fill up the crack. The healing agent is then polymerized and mends the cracks (Koh et al., 2013)	13
Figure 2.4	Classification of inhibitors	14
Figure 2.5	Schematic representation of the fabrication of an LbL assembled nanoreservoir	17
Figure 2.6	Model of GO depicted by past researchers	23
Figure 2.7	Shapes and morphologies that can be tailored with GO	25
Figure 2.8	ALA, linolenic acid, C18:3 cis, cis, cis-9,12,15-octadecatrienoic acid Polyunsaturated Omega-3 (Kolodziejczyk et al., 2012)	32
Figure 2.9	difference between classical and Pickering emulsion (Chevalier & Bolzinger, 2013)	35
Figure 3.1	Flow chart of summarized experimental activities from raw materials characterization until the preparation of coating sample.	62
Figure 4.1	Raman spectra of GO	64
Figure 4.2	Particle size distribution of GO	65
Figure 4.3	SEM and TEM micrographs of GO sheet	66

Figure 4.4	Digital image of the emulsions formed with different disperse speed a) 400 rpm, b) 800 rpm, c) 1200 rpm, d) 1600 rpm, e) 2000 rpm, and f) 2400 rpm	68
Figure 4.5	Digital images of emulsions containing GOMs prepared with varied disperse speed monitored after 24 hours, a) 800rpm, b) 1200rpm, c) 1600rpm, d) 2000rpm, and e) 2400rpm	68
Figure 4.6	Image of the emulsion under optical microscope equipped with polarized light a) 400 rpm, b) 800 rpm, c) 1200 rpm, d) 1600 rpm, e) 2000 rpm, f) 2400 rpm g) single GOM under polarized light and h) single GOM without polarized light	71
Figure 4.7	Emulsion preparation, b) Breaking of linseed oil into small droplets by the propeller, c) GO sheets assembled themselves around the linseed oil droplets, d) stabilized Pickering emulsion (GOMs).	72
Figure 4.8	Droplet size distribution of GOMs, a) 400 rpm, b) 800 rpm, c) 1200 rpm and d) 1600 rpm	73
Figure 4.9	Average size distribution based on POM images and PSA of the emulsions	74
Figure 4.10	Digital image of the emulsions formed with different solid nanoparticles concentration a) 1.0 mg/ml, b) 3.7 mg/ml, c) 5.0 mg/ml, d) 7.0 mg/ml, and e) 1.0 mg/ml after few minutes	76
Figure 4.11	Digital images of emulsions containing GOMs prepared with varied solid particles concentration monitored after 24 hours, a) 1.0 mg/ml b) 5.0 mg/m and c) 7.0 mg/ml	77
Figure 4.12	POM images of the emulsions formed with different solid nanoparticles concentration a) 1.0 mg/ml, b) 3.7 mg/ml c) 5.0 mg/ml, and d) 7.0 mg/ml	78
Figure 4.13	Droplet size distribution, a) 1.0 mg/ml, b) 3.7 mg/ml, c) 5.0 mg/ml, d) 7.0 mg/ml	80
Figure 4.14	Average size distribution based on POM images and PSA of the emulsions	81
Figure 4.15	GOMs, b) GOMs after 21 days, stored at room temperature.	82
Figure 4.16	FTIR spectra of GO, LO, and GOMs	84
Figure 4.17	Thermogram of linseed oil (black) and GOMs (coloured, done thrice)	85

Figure 4.18	TEM micrograph of GOMs	86
Figure 4.19	POM images of GOMs dispersed in polar solvent and alcohol, a) acetone, b) ethanol	88
Figure 4.20	POM images of GOMs mixed with various coating matrix, a) SB epoxy, b) WB epoxy and c) waterborne amine-adduct curing agent.	90
Figure 4.21	FTIR spectra of GO, amine-adduct curing agent and GO added amine-adduct curing agent	93
Figure 4.22	POM images of GOMs mixed with various coating matrix, a) SB epoxy, b) acrylic emulsion, c) WB epoxy, d) waterborne amine-adduct curing agent.	93
Figure 4.23	Possible reaction between GO and amine groups in curing agent of waterborne epoxy coating; a) Pristine GO, b) and c) possible reaction between amine-adduct curing agent with GO. The reaction took place on the carboxylic and epoxide sites of the GO sheets	94
Figure 4.24	Proposed destabilization mechanism - The existence of the amine group in curing agent destabilizes the GOMs. Strong covalent bond detaches the individual GO sheet from its assemblies, which is mainly held by weak Van-der-Waals attraction.	95
Figure 4.25	Chemical structure of D-2000. The amine group attached at both ends plays an important role in stitching the GO sheets.	97
Figure 4.26	FTIR spectra of GO, amine-stitched GOMs shell and D-2000	97
Figure 4.27	Schematic representation of how the amine group hold the GO sheets, creating 'stitch'	98
Figure 4.28	POM images of amine-stitched GOMs dispersed in polar solvent and alcohol, a) acetone, b) ethanol	100
Figure 4.29	OM images of different wt% amine-stitched GOMs (red arrow) in cured WB epoxy coating, a) 5wt%, b) 10wt%, c) 15wt%, and d) 20wt%	102
Figure 4.30	XRD pattern of neat epoxy and GOMs loaded epoxy coating	104
Figure 4.31	Images of adhesion of GOMs loaded epoxy coatings, a) pure, b) 5wt% GOMs, c) 10wt% GOMs, d) 15wt% GOMs and e) 20wt% GOMs	105

Figure 4.32	Digital image of waterborne epoxy coating with a varied amount of GOMs after 24 hours immersed in 3.5% NaCl solution, a) pure epoxy, b) 5wt%, c) 10wt%, d) 15wt%, and e) 20 wt%	107
Figure 4.33	Digital image of wet (left) and dried (right) waterborne epoxy coating with varied wt% GOMs after 720 hours immersed in 3.5% NaCl solution, the yellow arrow indicates the evolution of corrosion, a) pure epoxy, b) 5wt%, c) 10wt%, d) 15wt% and e) 20 wt%	109
Figure 4.34	Anticorrosion mechanism of the coating	110
Figure 4.35	The relationship between the swelling degree and corrosion rate	112
Figure 4.36	Digital image of waterborne epoxy coating on carbon steel substrate with varied GOMs loading after 24 hours salt spray test, a) pure epoxy, b) 5wt%, c) 10wt%, d) 15wt% and e) 20 wt%	114
Figure 4.37	Digital image of WB epoxy coating on carbon steel substrate with 10wt% GOMs loading immersed in 5 wt% NaCl solution, a) before immersion and b) after 24 hours immersion	114
Figure 4.38	3D optical microscope images of the scratched area after 120 hours, a) neat epoxy, b) 5 wt% GOMs, c) 10 wt% GOMs, d) 15 wt% GOMs, and e) 20 wt% GOMs	117
Figure 4.39	POM images of different wt% of silica in 10 wt% GOMs (red arrow) loaded epoxy coating, a) 1wt%, b) 3wt%, and c) 5wt%	119
Figure 4.40	XRD pattern of GOMs loaded epoxy and GOMs-Silica loaded epoxy coating	120
Figure 4.41	Images of adhesion of GOMs-silica loaded epoxy coatings, a) 1 wt% silica, b) 3wt% silica, and c) 5 wt% silica	121
Figure 4.42	Digital image of GOMs loaded epoxy coating with a varied amount of silica after 24 hours immersed in 3.5% NaCl solution, a) 1 wt%, b) 3 wt% and, c) 5wt%	122
Figure 4.43	Digital image of wet (left) and dried (right) GOMs loaded waterborne epoxy coating with varied wt% silica after 720 hours immersed in 3.5% NaCl solution, a) 1 wt%, b) 3 wt%, and c) 5 wt%	124
Figure 4.44	Peeling of the coating layer (red circle). Trace of corrosion was not observed under the peeled region a) 3wt% and b) 5 wt%	124

Figure 4.45	Carbon steel sample with 10 wt% GOMs and 1 wt% silica subjected to immersion test in 3.5% NaCl, a) before immersion, and b) after 96 hours immersion	125
Figure 4.46	The relationship between the swelling degree and corrosion rate	126
Figure 4.47	3D optical microscope images of the scratched area after 120 hours, a) 1 wt% silica, b) 3 wt% silica, and c) 5 wt% silica	128



LIST OF SYMBOLS

%	percentage
~	approximate
\leq	less than or equal to
\geq	more than or equal to
°	degree
° C	degree celcius
\$	dollar
λ	wavelength
μm	micrometer
Ca	capillary action
cm	centimeter
cm^{-1}	reciprocal centimeter
cm^2	squared centimeter
C_v	coefficient of variation
g	gram
g^{-1}	reciprocal gram
GPa	gigapascal
g/L	gram per liter
Hg	hectogram
hr	hour
K^{-1}	reciprocal Kelvin
m^{-1}	reciprocal meter

mg	milligram
mg/ml	milligram per milliliter
min	minute
min ⁻¹	reciprocal minute
ml	milliliter
mm	millimeter
nm	nanometer
rpm	rotation per minute
s	second
T _g	glass transition temperature
TPa	terapascal
V	volt
wt %	weight percentage
W	watt
θ	theta
θ _w	contact angle

LIST OF EQUATIONS

Equation 2.1	Capillary number, Ca	37
Equation 2.1	Coefficient of variation, C_v	53
Equation 2.1	Bragg's Law	57
Equation 2.1	Adhesion percentage	59
Equation 2.1	Corrosion rate	59
Equation 2.1	Stokes equation	75
Equation 2.1	Number of microcapsules, N	84
Equation 2.1	Total surface area of GOMs	84
Equation 2.1	Thickness of GOM's shell	85
Equation 2.1	Laplace equation	113

LIST OF ABBREVIATIONS

2D	two dimensional
Al ₂ O ₃	aluminum (ii) oxide
ALA	α -linolenic acid
APTES	(3-aminopropyl)triethoxysilane
ASTM	american society of testing and materials
BTA	benzotriazole
C	carbon
C=C	compound containing alkene group
CAGR	compound annual growth rate
CNT	carbon nanotube
Cr	chromium
C-OH	compound containing aldehyde group
-COOH	compound containing carboxyl group
D-2000	poly(propylene glycol) bis(2-aminopropyl ether)
DCPD	dicyclopentadiene
DMF	dimethylformamide
e ⁻	electrons
EC	ethyl cellulose
EI	emulsion index
EIS	electrochemical impedance spectroscopy
EN	electrochemical noise
fGO	functionalized graphene oxide

$f\text{SiO}_2$	functionalized silica
Fe	iron
$\text{Fe}(\text{OH})_2$	iron hydroxide
Fe^{2+}	iron ion lack of 2 electrons
$\text{Fe}_2\text{O}_3 \cdot \text{H}_2\text{O}$	hydrated iron hydroxide
Fe_3O_4	iron (iii) oxide
FT-IR	fourier transform infrared
GDP	gross domestic product
GO	graphene oxide
GOMs	graphene oxide microcapsules
GONs	graphene oxide nanosheets
H_2O	water
HMIM	1-hexyl-3-methylimidazolium chloride
HNTs	halloysite clay nanotubes
ICP-MS	inductively coupled plasma mass spectrometry
IMPACT	international measures of prevention, application, and economics of corrosion technologies
LbL	layer-by-layer
LDPE	low-density polyethylene
M_n	molecular number
Mn	manganese
MSNs	mesoporous silica nanoparticles
NACE	national association of corrosion engineers
NaCl	sodium chloride

NMP	n-methylpyrrolidone
NPS	nanoparticles
NS	nanosheet
O/W	oil-in-water
O ₂	oxygen gas
OH	hydroxide
OH ⁻	hydroxide ion
P	phosphorus
PANI	polyaniline
PBAR	plant-based alkyd resin
PEI	polyethyleneimine
PEO	plasma electrolytic oxidation
PET	polyethylene terephthalate
PI	polyimides
PMMA	polymethyl methacrylate
POM	polarized optical microscope
PSA	particle size analyzer
PSS	polystyrene sulfonate
PU	polyurethane
PUF	poly(urea-formaldehyde)
PVA	poly-vinyl alcohol
rGO	reduced graphene oxide
RGONs	reduced graphene oxide nanosheets
S	sulfur

SAC	sulfanilic acid azocromotrop
SB	solvent-based
SEM	scanning electron microscope
Si	silicon
SiO ₂	silica / silicon dioxide
TEM	transmission electron microscope
TGA	thermogravimetric analysis
THF	tetrahydrofuran
TiO ₂	titania/titanium dioxide
TNTs	titanium dioxide nanotubes
TRGO	thermally reduced graphene oxide
UF	urea-formaldehyde
W/O	water-in-oil
WB	waterborne
XRD	x-ray diffractometer
ZnO	zinc oxide
ZrO	zirconium oxide

CHAPTER ONE

INTRODUCTION

1.1 BACKGROUND OF THE STUDY

Corrosion is always being the major reason for energy and material loss. Many researchers are still bewildered on how to overcome the corrosion in steel structure, especially in oil and gas industries where the metal structure is exposed to the moist and aggressive environment. The behaviors of materials in such environment have urged both researchers and scientists to find a good solution to solve this problem. Hence, a layer of corrosion-resistant coating is the most effective way, as the coating act as the intermediate surface between the metal substrate and the environment, protecting against erosion and corrosion (Metal Coatings Corporation, 2016). But, the conventional coatings only give a slight improvement in the properties of the substrate as they are made up of micron-scale substances. Solidification of conventional coating also leads to a few defects such as micro-pores and bubbling (He et al., 2015). Also, they are easy to crack (Cotting & Aoki, 2015). Besides the infamous nanocoating, which possesses excellent physical, mechanical, thermal, and chemical properties, the utilization of smart coating is another great alternative.

Smart coating is a new generation coating transcending the conventional coating and other functional materials. Rather than act as a rigid barrier between the substrate and the environment, which is what conventional coatings did, smart coatings are designed to respond to the environment and, through that response, enhance the coating's service life and functionality (I. S. Cole, 2014). It is also frequently used interchangeably with self-healing coating (Hughes et al., 2016).